JOURNAL OF MOLECULAR RECOGNITION
J. Mol. Recognit. 2000;**13**:27–34

Conformations of nicotinamide adenine dinucleotide (NAD^+) in various environments

Paul E. Smith[1] and John J. Tanner[2]*

[1]Department of Biochemistry, Kansas State University, Manhattan, KS 66506-3702, USA
[2]Department of Chemistry, University of Missouri–Columbia, Columbia, MO 65211, USA

Enzymes bind NAD^+ in extended conformations and yet NAD^+ exists in aqueous solution as a compact, folded molecule. Thus, NAD^+ conformation is environment dependent. In an attempt to investigate the effects of environmental changes on the conformation of NAD^+, a series of molecular dynamics simulations in different solvents was performed. The solvents investigated (water, DMSO, methanol and chloroform) represented changes in relative permittivity and hydrophobic character. The simulations predicted folded conformations of NAD^+ to be more stable in water, DMSO and methanol. In contrast, extended conformations of NAD^+ were observed to be more stable in chloroform. Furthermore, the extended conformations observed in chloroform were similar to conformations of NAD^+ bound to enzymes. In particular, a large separation between the aromatic rings and a strong interaction between the pyrophosphate and nicotinamide groups were observed. The implications of these observations for the recognition of NAD^+ by enzymes is discussed. It is argued that a hydrophobic environment is important for stabilizing unfolded conformations of NAD^+. Copyright © 2000 John Wiley & Sons, Ltd.

Keywords: **NAD, nicotinamide adenine dinucleotide; molecular dynamics simulation; chloroform; methanol; water; DMSO; solvation; folding/unfolding equilibria**

Received 22 July 1999; revised 13 October 1999; accepted 13 October 1999

INTRODUCTION

One of the most common molecular recognition events in living systems is the binding of nicotinamide adenine dinucleotide (NAD) to an enzyme. NAD is a major unit of currency in biological redox chemistry. Over 100 NAD-dependent dehydrogenases are known, such as those that catalyze the oxidation of glyceraldehyde-3-phosphate, ethanol, lactate and malate. In these enzymes, the oxidized form of NAD (NAD^+) is reduced by accepting a hydride ion at the nicotinamide C4 position. The reduced form of NAD (NADH) provides the reducing electrons for mitochondrial ATP production. NADH is also a substrate for NADH oxidase/flavin reductase enzymes (Koike *et al.*, 1998; Lei *et al.*, 1994; Lei and Tu, 1994; Zenno *et al.*, 1996a,b), which produce reduced flavin for the bacterial luciferase light emitting reaction, among other roles (Tu and Mager, 1995). In addition to its redox function, NAD^+ is a labile substrate for ADP ribosylating enzymes, which cleave the nicotinamide glycosyl bond (Althaus and Richter, 1987; Jacobson and Jacobson, 1989). NAD is of practical importance because analogs of this molecule are potentially useful as anticancer (Franchetti *et al.*, 1998; Konno *et al.*, 1991; Nagai *et al.*, 1991), antibacterial (Zhang *et al.*, 1999), and antitrypanosomal agents (Aronov *et al.*, 1998; Van Calenbergh *et al.*, 1995; Verlinde *et al.*, 1994a,b).

NAD^+ binding to enzymes is an interesting molecular recognition problem for two reasons. First, with over a dozen rotatable bonds, NAD^+ is a flexible substrate that can adopt different conformations depending on its environment. Second, NAD^+ displays a diverse set of functional groups, including a hydrophobic ring system (adenine), formal positive (nicotinamide ring) and negative (pyrophosphate) charges, and hydrogen bonding groups (ribose hydroxyl groups, carboxamide). This combination of flexibility and chemical diversity means that NAD^+ can accommodate a wide range of active site shapes and it has the potential to form favorable interactions with the entire repertoire of naturally occurring amino acids. Furthermore, NAD^+ can form intramolecular interactions that mimic the intermolecular interactions that stabilize enzyme–NAD^+ complexes, including electrostatic attraction, hydrophobic contacts and aromatic ring stacking.

The effect of environment on NAD^+ conformation is significant. NAD^+ in aqueous solution adopts compact, folded conformations in which the distance between the nicotinamide and adenine rings is 0.4 –0.5 nm (Catterall *et al.*, 1969; Ellis *et al.*, 1973; Jardetzky and Wade-Jardetzky, 1966; McDonald *et al.*, 1972; Meyer *et al.*, 1962; Miles and Urry, 1968; Oppenheimer *et al.*, 1971; Riddle *et al.*, 1976; Sarma *et al.*, 1968; Smith and Tanner, 1999; Velick, 1958; Weber, 1957; Zens *et al.*, 1975, 1976). In contrast, NAD^+ bound to enzymes adopts extended conformations in which the nicotinamide and adenine rings are separated by 1.2–1.5 nm. Perhaps the most recognizable example of an

* Correspondence to: John J. Tanner, Department of Chemistry, University of Missouri-Columbia, Columbia, MO 65211, USA.
E-mail: tannerjj@missouri.edu
Contract/grant sponsor: Kansas Agricultural Experimental Station.
Contract/grant sponsor: Big 12 Faculty Fellowship Award from the University of Missouri–Columbia.

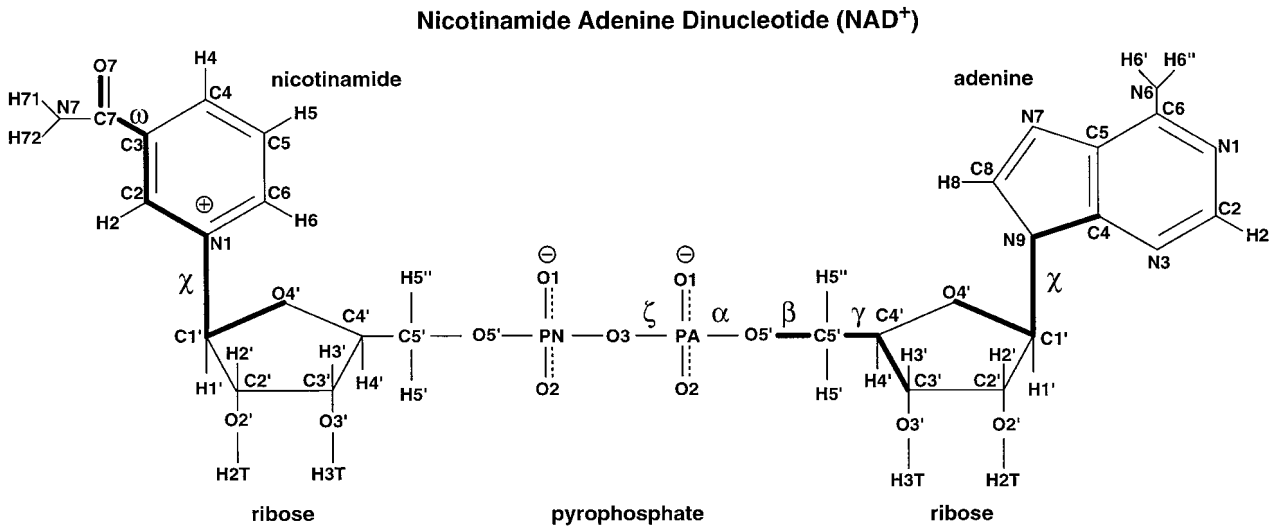

Figure 1. Chemical structure and nomenclature of NAD^+. Dihedral angles are noted by Greek letters. The thick bonds indicate the dihedral angle definitions for γ, χ and ω.

extended NAD^+ is that bound to a pair of mononucleotide-binding (or Rossmann fold) domains, in which each half of the coenzyme binds to a pair of $\beta-\alpha-\beta$ motifs (Brändén and Tooze, 1991). The only exception to this paradigm is the crystal structure of flavin reductase P (FRP) from *Vibrio harveyi* (Tanner *et al.*, 1999). NAD^+ is an inhibitor of FRP and it adopts a novel folded conformation in which the nicotinamide and adenine rings stack in parallel with an inter-ring distance of 0.36 nm. NAD^+ appears to inhibit FRP by adopting a catalytically unproductive conformation in which the nicotinamide C4 and its hydride transfer partner are separated by 1 nm. The FRP/NAD^+ crystal structure showed, for the first time, that it is possible for a protein surface to recognize and bind a highly compact, folded NAD^+ (Tanner *et al.*, 1999), and it is further demonstration of the conformational diversity of NAD^+.

The fact that NAD^+ is folded in solution and extended during catalysis suggests that unfolding of the dinucleotide might be an important feature of NAD^+ recognition, and refolding might be important for product release. Little is known about the energetics and dynamics of these processes, nor is it known how, or even if, the enzyme assists in the unfolding and folding of the dinucleotide.

The present calculations were undertaken to address the question of how the protein environment facilitates the unfolding of NAD^+ from its compact aqueous solution conformation to a catalytically competent, extended conformation. A commonality among proteins is that they present a non-aqueous surface to substrates, therefore, simulations of NAD^+ in solvents with various dielectric constants and hydrophobic character were performed in order to identify basic elements of NAD^+ recognition by proteins.

METHODS

Classical molecular dynamics simulations of NAD^+ (Fig. 1) in explicit solvent were performed. Explicit solvent was used to provide the most accurate description of solvent effects (Cheatham and Brooks, 1998; Smith and Pettitt, 1994). Solvents considered were water, dimethylsulfoxide (DMSO), methanol and chloroform. Atom naming conventions and dihedral angle definitions are indicated in Fig. 1. All four simulations proceeded from the same initial solute conformation and were performed for a total of 5.1 ns, including 0.1 ns of equilibration. Following our initial studies (Smith and Tanner, 1999), the folded conformation of NAD^+ obtained from the FRP/NAD^+ crystal structure (Tanner *et al.*, 1999) was used as the initial conformation in all four simulations.

The force field of Pavelites *et al.* (1997) was used for NAD^+. Solvent force fields were taken from the literature: TIP3P water model (Jorgensen *et al.*, 1983), DMSO (Liu *et al.*, 1995), methanol (Jorgensen, 1986), and chloroform (Tironi and van Gunsteren, 1994). NAD^+ was solvated by placing in a pre-equilibrated cubic box of solvent molecules, and removing water, DMSO, methanol or chloroform molecules in which the central solvent atom was within 0.2, 0.35, 0.2 or 0.35 nm, respectively, from any non-hydrogen atom of the solute. The initial systems contained one NAD^+ plus solvent molecules in a box of length 3.0 nm. Each system was minimized with 100 steps of steepest descent and then equilibrated for 0.1 ns. For the first 0.05 ns of the equilibration the masses of the solute atoms were increased by a factor of 10 to ensure preferential equilibration of the solvent molecules, and velocities were reassigned every 1 ps to avoid local heating artifacts. None of the energy terms from any of the simulations displayed a discernible drift with time after the initial equilibration period. The setup and results of the simulations are summarized in Table 1.

Simulations were performed in the NPT ensemble at 300K and 1 atm using the weak coupling technique to modulate the temperature and pressure (van Gunsteren and Berendsen, 1990) with relaxation times of 0.1 and 0.5 ps, respectively. SHAKE (Ryckaert *et al.*, 1977) was used to constrain all bonds with a relative tolerance of 10^{-4},

Table 1. Summary of MD simulations[a]

	Water	DMSO	Methanol	Chloroform
Number of solvent molecules	867	222	374	198
Volume (nm^3)	26.233	26.064	27.332	27.010
NAD$^+$ energy (kJ/mol)	−1101	−1157	−1157	−1360
Solvent energy (kJ/mol)	−35101	−11637	−12780	−1763
NAD$^+$-solvent energy (kJ/mol)	−1274	−945	−1066	−477
k-Space energy (kJ/mol)	113	162	150	102
Experimental relative permittivity	79	46	33	5

[a] Averages over 5 ns of simulation in the NPT ensemble with $P = 1$ atm and $T = 300$K. Experimental relative permittivities of water, methanol, and chloroform were taken from Weast (1975). The value for DMSO was obtained from Liu *et al.* (1995).

allowing a 2 fs time step. Configurations and energies were saved every 0.1 ps for analysis.

Electrostatic interactions were calculated using the Ewald technique (de Leeuw *et al.*, 1980) using a convergence parameter of 2.5 nm^{-1}, a real space cutoff of 1.2 nm, and including all lattice vectors with $n^2 \leq 64$. In order to avoid possible problems associated with simulating a charged Ewald system (Bogusz *et al.*, 1998), the solute was neutralized by the addition of a unit positive charge, equally partitioned over all 70 NAD$^+$ atoms. Similar approaches have been used previously (Northrup *et al.*, 1981; van Gunsteren and Berendsen, 1987). Charge neutralization required only a small adjustment of + 0.0143 *e* to each atomic charge and the validity of this approach was confirmed in previous NAD$^+$ simulations (Smith and Tanner, 1999). Ewald artifacts are expected to be small for the high permittivity solvents (Huenenberger and McCammon, 1999; Smith and Pettitt, 1996), and to possibly favor folded conformations in chloroform (Huenenberger and McCammon, 1999).

Analysis of interaction energies and accessible surface areas was performed on a group basis. Groups were defined by the sets of atoms that are isolated after breaking the following bonds: N1–C1′N, C5′N–O5′N, O5′A–C5′A and C1′A–N9. The five resulting groups were denoted as N (nicotinamide), R_N (nicotinamide ribose), P (pyrophosphate), R_A (adenine ribose), and A (adenine). The interaction energies between different groups were obtained using the van der Waals energy and the standard Coulomb potential (not the Ewald potential). The latter approximation was used to circumvent the problem of deconvoluting the reciprocal space term into atom–atom interactions (Allen and Tildesley, 1987). Accessible surface area (ASA) calculations were performed using X-plor (Brünger, 1992) with a probe radius of 0.14 nm and a grid accuracy of 0.025. Inter-ring distances were based on the centroids of the six-membered nicotinamide ring (N1, C2, C3, C4, C5, C6) and the nine-membered adenine ring system (N1, C2, N3, C4, C5, C6, N7, C8, N9).

The following crystal structures used in the analysis were obtained from the Protein Data Bank (Abola *et al.*, 1987): flavin reductase P, ID 2BKJ (Tanner *et al.*, 1999); glyceraldehyde-3-phosphate dehydrogenase, ID 1CER (Tanner *et al.*, 1996); malate dehydrogenase, ID 1BMD (Kelly *et al.*, 1993); NADH peroxidase, ID 2NPX (Stehle *et al.*, 1993); alcohol dehydrogenase, ID 2OHX (Eklund *et al.*, 1982); 3-isopropylmalate dehydrogenase, ID 1HEX (Hurley and Dean, 1994); and diphtheria toxin, ID 1TOX (Bell *et al.*, 1997). All calculations were performed after removing non-NAD$^+$ atoms from the PDB files.

RESULTS

The time histories of the nicotinamide–adenine inter-ring distances for the four simulations are shown in Fig. 2. For the water simulation, the time history can be divided into three main regions, $t = 0$ –1.7 ns, $t = 1.7$ –2.5 ns, and $t = 2.5$ –5.0 ns. The first time slice was dominated by conformations similar to that of the FRP crystal structure. The initial

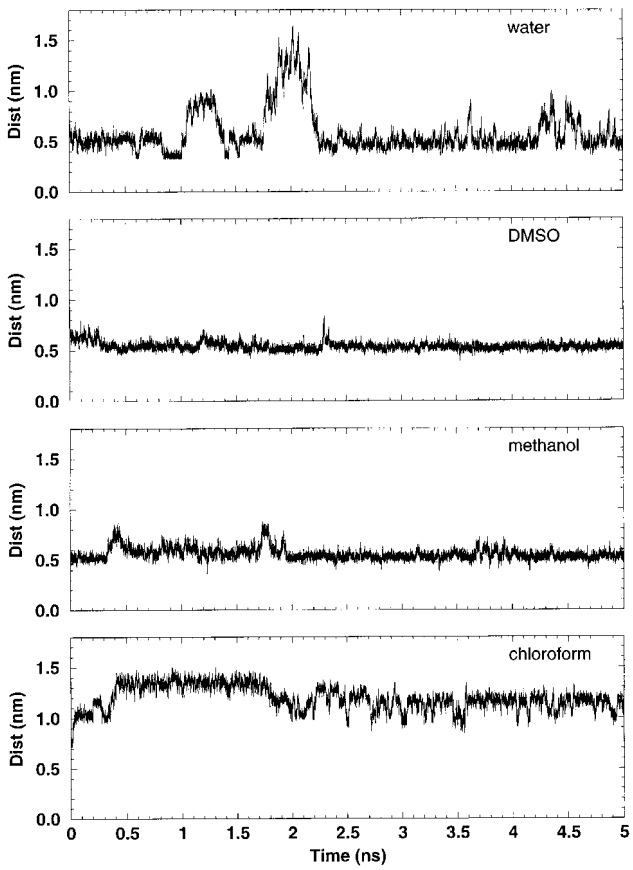

Figure 2. Time histories of the inter-ring distance for each simulation.

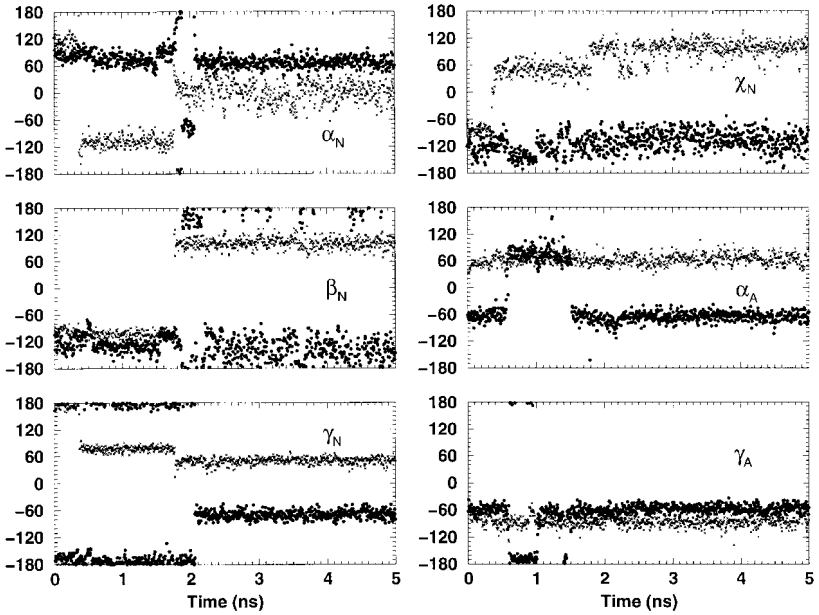

Figure 3. Time histories of various dihedral angles obtained from the water (dots) and chloroform (crosses) simulations.

NAD^+ conformation persisted for the first 1 ns of the simulation, followed by an unfolding transition to a moderately extended conformations at 1.1–1.3 ns, and a return to the initial conformation. The second time slice was characterized by complete unfolding of the molecule into highly extended conformations (t = 1.9–2.2 ns), followed by refolding into a compact conformation that was different from the initial conformation. During the final 2.5 ns of the simulation, the new folded conformation persisted, along with other moderately extended conformations resulting from unfolding events near t = 4.3 and 4.5 ns.

The water simulation and the final stable conformation that results has been discussed in detail elsewhere (Smith and Tanner, 1999). To summarize, the predominant form of NAD^+ in water is a folded conformation characterized by a nicotinamide–adenine inter-ring distance of 0.52 nm, an angle of 148° between the aromatic ring planes, parallel glycosyl bond vectors, and the nicotinamide B side facing the adenine ring (Plate 1, water). The inter-ring distance and non-parallel arrangement of the aromatic rings are consistent with NMR data (Riddle *et al.*, 1976; Zens *et al.*, 1975, 1976), while the interaction of the nicotinamide B side with adenine is in agreement with several experimental studies (Miles and Urry, 1968; Oppenheimer *et al.*, 1971; Sarma *et al.*, 1968). The final folded conformation is favored over the initial folded one because of the increased solvation of the charged nicotinamide ring (Smith and Tanner, 1999).

The conformations obtained in the non-aqueous solvents were significantly different from the predominant form in water (plate 1). The effect of DMSO and methanol on the initial conformation was small in comparison to the effect of water. The inter-ring distance increased slightly in the DMSO and methanol simulations, corresponding to an unstacking of the two aromatic rings, but the overall conformation of the molecule remained close to the starting structure. However, in chloroform the solute readily unfolded to separate both aromatic rings, and adopted conformations similar to those observed for NAD^+ bound to proteins.

Representative structures from the four simulations are displayed in Plate 1, together with the initial structure (FRP, PDB ID 2BKJ) and a conformation from a Rossmann fold enzyme, glyceraldehyde-3-phosphate dehydrogenase (PDB ID 1CER) (Tanner *et al.*, 1996). There are several similarities between the Rossmann fold NAD^+ structure and the conformation obtained in the chloroform simulation. The large aromatic ring separation and close proximity of the pyrophosphate and nicotinamide groups are particularly striking.

The major NAD^+ conformations from the chloroform simulation are compared with two conformations from the protein data bank in Plate 2. The four structures have two features in common. First, the adenine has high exposure to the environment. Second, there are hydrogen bonds between the carboxamide and pyrophosphate groups. The nicotinamide halves of 1CER and the t = 1 ns MD conformation superimpose with a root mean square difference (RMSD) of 1.1 Å, while the RMSD between 1CER and the t = 4 ns conformation is 0.9 Å. The corresponding RMSD values for the 1TOX conformation are 1.2 and 1.5 Å for t = 1 ns and t = 4 ns, respectively. Obviously, the hydrogen bonding interaction is facilitated by the low relative permittivity of chloroform, which cannot shield the electrostatic interaction between the two groups. This is clearly not such an important factor for the other solvent systems considered here, which did not display a direct interaction between these two groups The dihedral transitions associated with the conformational changes of NAD^+ in water and chloroform are displayed in Fig. 3. There were many transitions during both simulations, suggesting that a significant number of distinct NAD^+ conformations had been sampled

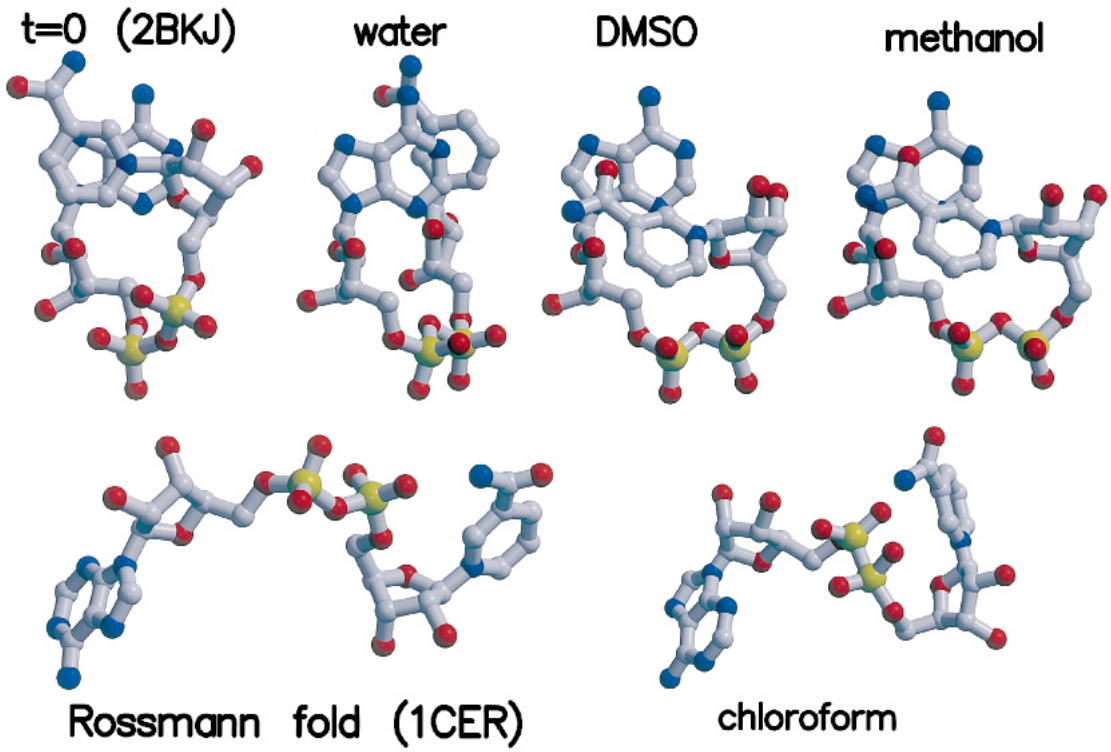

Plate 1. Representative structures of NAD^+ from each simulation (extracted at *t*=4 ns) compared to the initial structure (2BKJ) and NAD^+ from a Rossmann fold enzyme, glyceraldehyde-3-phosphate dehydrogenase (1CER). Figure prepared with Molscript (Kraulis, 1991).

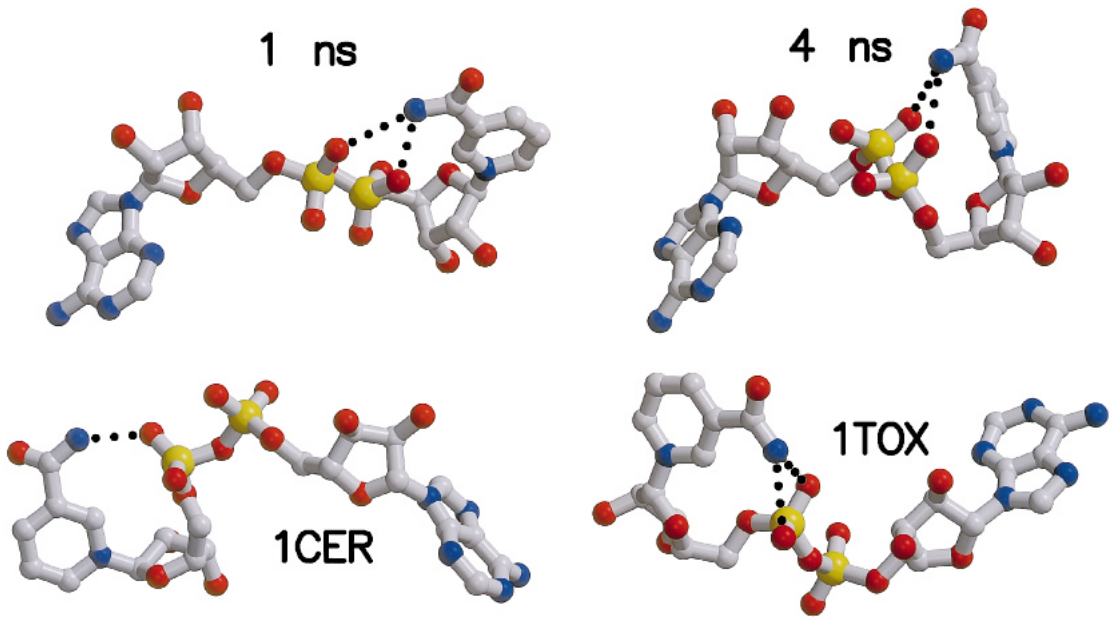

Plate 2. Comparison of the two predominant structures obtained in chloroform with the conformations of NAD^+ bound to a Rossmann fold enzyme, glyceraldehyde-3-phosphate dehydrogenase (1CER) and diptheria toxin (1TOX). The dotted lines represent interactions within 0.35 nm. Figure prepared with Molscript (Kraulis, 1991).

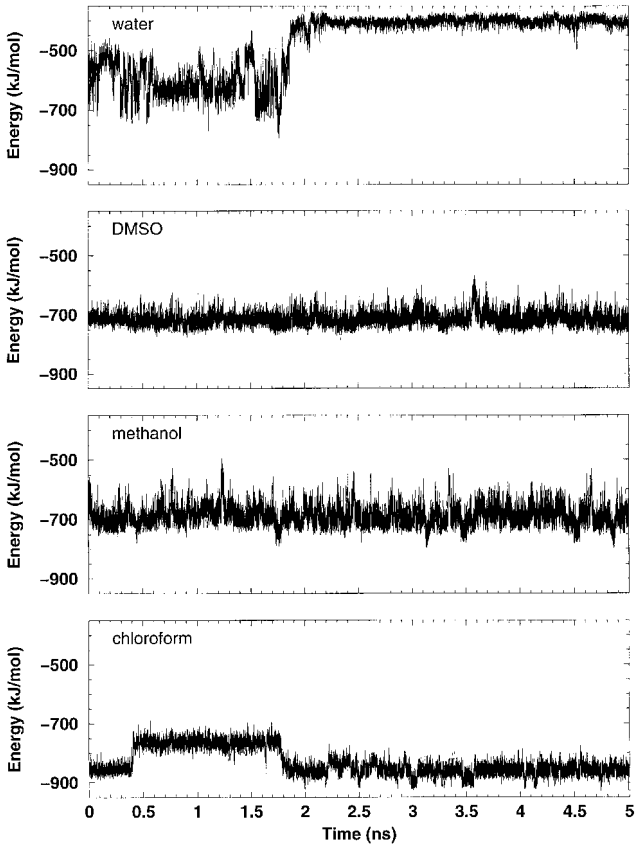

Figure 4. Time histories of the interaction energy between the pyrophosphate and nicotinamide groups obtained from each simulation.

and that the results presented here are indicative of those for an equilibrium system. In addition to the types of dihedral transitions observed in water, the chloroform simulation resulted in transitions around the χ_N dihedral. This is required to facilitate a direct interaction between the carboxamide and the phosphate groups.

The effect of the different solvents on the interactions between the two charged groups of NAD^+ is illustrated in Fig. 4, where the time histories of the interaction energy between the pyrophosphate and nicotinamide groups are displayed. The average interaction energies obtained from the latter stages of each simulation follow the trend expected based on their relative permittivities. The low dielectric chloroform solvent resulted in the most favorable interaction energy, while the high dielectric water solvent possessed a relatively small interaction energy.

A comparison between the average properties of NAD^+ in chloroform and those displayed by enzyme-bound NAD^+ is summarized in Table 2. The crystal structures used in Table 2 represent the major classes of NAD^+ binding protein folds identified by Bell and coworkers (Bell *et al.*, 1997). The interaction energies for the NAD^+ molecules were obtained using the same force field parameters as used for the simulations. Examination of the different interaction energies does not provide any indication of a general trend in NAD^+ bound conformations. The total potential energies of the PDB conformations are typically less favorable than those of the MD conformations, while the pyrophosphate–nicotinamide interaction energies of the PDB conformations vary between the water and DMSO/methanol values. The inter-ring distances of enzyme-bound NAD^+ are large, due to the extended nature of NAD^+ in these systems. This is also mirrored in the radius of gyration data. Both the inter-ring distance and the radius of gyration data compare well with the structure of NAD^+ in chloroform solution. The accessible surface area of NAD^+ is higher for the conformations bound to proteins, while it is lower and fairly independent of solvent during the simulations performed here. Examination of the group contributions to the accessible surface area obtained from the simulations suggests a compensation between the accessibility of the pyrophosphate and adenine groups in water and chloroform. The accessibility of the pyrophosphate group decreased moving from water to chloroform, whereas the accessibility of the adenine ring increased correspondingly.

Table 2. Properties of NAD^+ conformations from MD simulation and the PDB

	NAD^+ energy (kJ/mol)	P–N energy (kJ/mol)	R_g (nm)	N–A distance (nm)	NAD^+ ASA (nm^2)	P ASA (nm^2)	N ASA (nm^2)	A ASA (nm^2)
MD								
Water	−1125	−401	0.46	0.52	6.19	1.26	1.39	1.25
DMSO	−1313	−714	0.41	0.53	5.86	1.16	1.06	1.29
Methanol	−1320	−692	0.42	0.54	5.89	1.18	1.08	1.30
Chloroform	−1603	−860	0.51	1.14	6.49	0.81	1.33	1.59
PDB								
2BKJ	−1033	−527	0.43	0.39	6.1	1.4	1.2	1.2
1CER	−1087	−616	0.59	1.47	7.1	1.2	1.5	1.7
1BMD	−917	−443	0.60	1.37	7.3	1.3	1.6	1.7
2OHX	−1004	−477	0.62	1.46	7.3	1.3	1.6	1.7
2NPX	−1194	−530	0.62	1.54	7.2	1.2	1.6	1.7
1HEX	−1075	−491	0.61	1.41	7.1	1.2	1.6	1.5
1TOX	−1047	−626	0.54	1.20	6.9	1.1	1.5	1.6

DISCUSSION AND CONCLUSIONS

Simulations of NAD^+ in four solvents having different relative permittivities and hydrophobic character were performed to model the effect of environment on the conformation of NAD^+. These simulations were started from a folded form of the molecule that was determined by X-ray crystallography.

In DMSO and methanol no significant conformational changes occurred, although there was a slight increase in inter-ring distance relative to the initial structure. In water, a conformational transition to another folded form occurred. This conformation is consistent with several experimental studies of NAD^+ in aqueous solution (Smith and Tanner, 1999). In contrast, extended structures were produced in the chloroform simulation, characterized by large inter-ring distances and close proximity of the pyrophosphate and nicotinamide moieties.

Since the initial conformation appeared to be relatively stable in methanol and DMSO, it is tempting to conclude that these solvents might mimic some essential feature of the FRP active site, such as the polarity. However, the lack of conformational transitions precludes such a conclusion at this stage.

In water, the predominant folded conformation exhibits high exposure of the pyrophosphate to solvent and partial burial of the adenine. The opposite trend is observed in chloroform, i.e. burial of the pyrophosphate and exposure of the adenine, which results in an open conformation. This result is consistent with the low relative permittivity of chloroform, which results in a strong ionic interaction and low solvent accessibility of the pyrophosphate. Exposure of the adenine is also consistent with the hydrophobic character of chloroform and with the observation that adenine typically binds in a hydrophobic pocket in enzymes.

Crystal structures of enzyme-bound NAD^+ suggest that extension of the dinucleotide is required for catalysis (Bell *et al.*, 1997). Extended conformations have two main advantages over a folded conformation. First, an extended substrate exposes more surface area, thus, there are more sites available to interact with the enzyme. Second, by unfolding, NAD^+ reduces the excluded volume around the nicotinamide, thus allowing the nicotinamide to engage its hydride transfer partner with the correct orientation and at the required distance of less than 0.4 nm.

The extended structures in the chloroform simulation are similar to some NAD^+ conformations bound to Rossmann fold domains and diphtheria toxin. First, the adenine in these enzymes is buried in a hydrophobic pocket. Likewise, the adenine is fully exposed to a hydrophobic environment in the chloroform simulation. Second, in some enzyme-bound NAD^+ conformations there is substantial interaction between the nicotinamide and phosphate groups (Plate 2). This structural motif was also observed in the chloroform simulation.

It is interesting that a simple solvent such as chloroform can mimic two major features of NAD^+ binding to enzymes. This result suggests that, in addition to specific interactions such as shape complementarity, hydrogen bonding and ion pairing, the effective permittivity of the enzyme active site region might be important for the recognition of NAD^+ by enzymes. Specifically, exposure of NAD^+ to the hydrophobic surface of the enzyme contributes to the unfolding of NAD^+ during catalysis.

Finally, the nicotinamide –phosphate interaction observed in the chloroform simulation appears to be exaggerated relative to that seen in enzyme crystal structures. Competition from polar or charged protein residues would tend to weaken this intramolecular interaction, which would explain this difference. Alternatively, the relative permittivity of the chloroform model is only 2.4 (Tironi and van Gunsteren, 1994), which is a factor of two smaller than the experimental value (Weast, 1975), and this, coupled with possible Ewald artifacts (Huenenberger and McCammon, 1999), would also tend to slightly exaggerate the above interaction.

Acknowledgements

The authors would like to thank Alex Mackerell, Jr for making the NAD force-field parameters available. This project was partially supported by the Kansas Agricultural Experimental Station (Contribution 00-22-J, PES) and a Big 12 Faculty Fellowship Award from the University of Missouri-Columbia (JJT).

REFERENCES

Abola EE, Bernstein FC, Bryant SH, Koetzle TF, Weng J. 1987. Protein data bank. In *Crystallographic Databases — Information Content, Software Systems, Scientific Applications*; Allen FH, Bergerhoff G, Sievers R (eds); Data Commission of the International Union of Crystallography: Bonn; 107–132.

Allen MP, Tildesley DJ. 1987. *Computer Simulation of Liquids*; Oxford University Press: Oxford.

Althaus FR, Richter C. 1987. ADP-Ribosylation of Proteins. In *Molecular Biology, Biochemistry and Biophysics*, Vol. 37; Solioz M. (ed.); Springer, Berlin.

Aronov AM, Verlinde CL, Hol WG, Gelb MH. 1998. Selective tight binding inhibitors of trypanosomal glyceraldehyde-3-phosphate dehydrogenase via structure-based drug design. *J. Med. Chem.* **41**(24): 4790–4799.

Bell CE, Yeates TO, Eisenberg D. 1997. Unusual conformation of nicotinamide adenine dinucleotide (NAD) bound to diphtheria toxin: a comparison with NAD bound to the oxidoreductase enzymes. *Protein Sci.* **6**(10): 2084–2096.

Bogusz S, Cheatham TE, III Brooks BR. 1998. Removal of pressure and free energy artifacts in charged periodic systems via net charge corrections to the Ewald potential. *J. Chem. Phys.* **108**: 7070–7084.

Brändén C, Tooze J. 1991. *Introduction to Protein Structure*, Garland, New York.

Brünger AT. 1992. *X-PLOR Version 3.1 A System for X-ray Crystallography and NMR*, Yale University Press, New Haven.

Catterall WA, Hollis DP, Walter CF. 1969. Nuclear magnetic resonance study of the conformation of nicotinamide–adenine dinucleotide and reduced nicotinamide–adenine dinucleotide in solution. *Biochemistry* **8**(10): 4032–4036.

Cheatham TE, III, Brooks BR. 1998. Recent advances in molecular dynamics simulation towards the realistic representation of biomolecules in solution. *Theor. Chem. Acc.* **99**: 279–288.

de Leeuw SW, Perram JW, Smith ER. 1980. Simulation of electrostatic systems in periodic boundary conditions. I. Lattice sums and dielectric constants. *Proc. R. Soc., Lond. A* **373**: 27–56.

Eklund H, Plapp BV, Samama JP, Branden CI. 1982. Binding of substrate in a ternary complex of horse liver alcohol dehydrogenase. *J. Biol. Chem.* **257**(23): 14349–14358.

Ellis PD, Fisher RR, Dunlap RB, Zens AP, Bryson TA, Williams TJ. 1973. Nuclear magnetic resonance studies on pyridine dinucleotides. I. The pH dependence of the carbon 13 nuclear magnetic resonance of nicotinamide adenine dinucleotide. *J. Biol. Chem.* **248**(22): 7677–7681.

Franchetti P, Cappellacci L, Perlini P, Jayaram HN, Butler A, Schneider BP, Collart FR, Huberman E, Grifantini M. 1998. Isosteric analogues of nicotinamide adenine dinucleotide derived from furanfurin, thiophenfurin, and selenophenfurin as mammalian inosine monophosphate dehydrogenase (type I and II) inhibitors. *J. Med. Chem.* **41**(10): 1702–1707.

Huenenberger PH, McCammon JA. 1999. Ewald artifacts in computer simulations of ionic solvation and ion–ion interaction: a continuum electrostatics study. *J. Chem. Phys.* **110**: 1856–1872.

Hurley JH, Dean AM. 1994. Structure of 3-isopropylmalate dehydrogenase in complex with NAD+: ligand-induced loop closing and mechanism for cofactor specificity. *Structure* **2**(11): 1007–1016.

Jacobson MK, Jacobson EL. 1989. *ADP-Ribose Transfer Reactions. Mechanisms and Biological Significance*, Springer, New York.

Jardetzky O, Wade-Jardetzky NG. 1966. The conformation of pyridine dinucleotides in solution. *J. Biol. Chem.* **241**: 85–91.

Jorgensen WL. 1986. Optimized intermolecular potential functions for liquid alcohols. *J. Phys. Chem.* **90**: 1276–1284.

Jorgensen WL, Chandrasekhar J, Madura JD, Impey RW, Klein ML. 1983. Comparison of simple potential functions for simulating liquid water. *J. Chem. Phys.* **79**: 926–935.

Kelly CA, Bishiyama M, Ohnishi Y, Beppu T, Birktoft JJ. 1993. Determinants of protein thermostability observed in the 1.9-Å crystal structure of malate dehydrogenase from the thermophilic bacterium *Thermus flavus*. *Biochemistry* **32**: 3913–3922.

Koike H, Sasaki H, Kobori T, Zenno S, Saigo K, Murphy ME, Adman ET, Tanokura M. 1998. 1.8 A crystal structure of the major NAD(P)H:FMN oxidoreductase of a bioluminescent bacterium, *Vibrio fischeri:* overall structure, cofactor and substrate-analog binding, and comparison with related flavoproteins. *J. Mol. Biol.* **280**(2): 259–273.

Konno Y, Natsumeda Y, Nagai M, Yamaji Y, Ohno S, Suzuki K, Weber G. 1991. Expression of human IMP dehydrogenase types I and II in *Escherichia coli* and distribution in human normal lymphocytes and leukemic cell lines. *J. Biol. Chem.* **266**(1): 506–509.

Kraulis PJ. 1991. MOLSCRIPT: A program to produce both detailed and schematic plots of protein structures. *J. Appl. Crystallogr.* **24**: 946–950.

Lei B, Tu S-C, Eds. 1994. *Characterization of the Vibrio harveyi FMN:NADPH Oxidoreductase Expressed in Escherichia coli. Flavins and flavoproteins*. Edited by Yagi K. Berlin: Walter de Gruyter.

Lei B, Liu M, Huang S, Tu S-C. 1994. *Vibrio harveyi* NADPH:FMN oxidoreductase: cloning, sequence and overexpresssion of the gene, and purification and characterization of the cloned enzyme. *J. Bacteriol.* **176**: 3552–3558.

Liu H, Mueller-Plathe F, van Gunsteren WF. 1995. A force field for liquid dimethyl sulfoxide and physical properties of liquid dimethyl sulfoxide calculated using molecular dynamics simulation. *J. Am. Chem. Soc.* **117**: 4363–4366.

McDonald G, Brown B, Hollis D, Walter C. 1972. Some effects of environment on the folding of nicotinamide-adenine dinucleotides in aqueous solutions. *Biochemistry* **11**(10): 1920–1930.

Meyer WL, Mahler HR, Baker RH Jr. 1962. Nuclear magnetic resonance spectra and conformation of 1,4-dihydropyridines. *Biochim. Biphys. Acta* **64**: 353–358.

Miles DW, Urry DW. 1968. Reciprocal relations and proximity of bases in pyridine dinucleotides. *J. Biol. Chem.* **243**: 4181–4188.

Nagai M, Natsumeda Y, Konno Y, Hoffman R, Irino S, Weber G. 1991. Selective up-regulation of type II inosine 5′-monophosphate dehydrogenase messenger RNA expression in human leukemias. *Cancer Research* **51**(15): 3886–3890.

Northrup SH, Pear MR, Morgan JD, McCammon JA, Karplus M. 1981. Molecular dynamics of ferrocytochrome c. *J. Mol. Biol.* **153**: 1087–1109.

Oppenheimer NJ, Arnold LJ, Kaplan NO. 1971. A structure of pyridine nucleotides in solution. *Proc. Nat. Acad. Sci., USA* **68**(12): 3200–3205.

Pavelites JJ, Gao J, Bash PA, Mackerell AD. Jr. 1997. A molecular mechanics force field for NAD+, NADH, and the pyrophosphate groups of nucleotides. *J. Comput. Chem.* **18**: 221–239.

Riddle RM, Williams TJ, Bryson TA, Dunlap RB, Fisher RR, Ellis PD. 1976. Nuclear magnetic resonance studies on pyridine dinucleotides. 6. Dependence of the 13C spin–lattice relaxation time of 1-methylnicotinamide and nicotinamide adenine dinucleotide as a function of pD and phosphate concentration. *J. Am. Chem. Soc.* **98**(14): 4286–4290.

Ryckaert JP, Ciccotti G, Berendsen HJC. 1977. Numerical integration of the cartesian equations of motion of a system with constraints: molecular dynamics of *n*-alkanes. *J. Comput. Phys.* **23**: 327–341.

Sarma RH, Ross V, Kaplan NO. 1968. Investigation of the conformation of β-diphosphopyridine nucleotide (β-nicotinamide-adenine dinucleotide) and pyridine dinucleotide analogs by proton magnetic resonance. *J. Am. Chem. Soc.* **7**: 3052–3062.

Smith PE, Pettitt BM. 1994. Modeling solvent in biomolecular systems. *J. Phys. Chem.* **98**: 9700–9711.

Smith PE, Pettitt BM. 1996. Ewald artifacts in liquid state molecular dynamics simulations. *J. Chem. Phys.* **105**: 4289–4293.

Smith PE, Tanner JJ. 1999. Molecular dynamics simulations of nicotinamide adenine dinucleotide (NAD$^+$) in solution. *J. Am. Chem. Soc.* **121**: 8637–8644.

Stehle T, Claiborne A, Schulz GE. 1993. NADH binding site and catalysis of NADH peroxidase. *Eur. J. Biochem.* **211**(1–2): 221–226.

Tanner JJ, Hecht RM, Krause KL. 1996. Determinants of enzyme thermostability observed in the molecular structure of *Thermus aqaticus* D-glyeraldehyde-3-phosphate dehydrogenase at 2.5 Å resolution. *Biochemistry* **35**: 2597–2609.

Tanner JJ, Tu S-C, Barbour LJ, Barnes CL, Krause KL. 1999. Unusual folded conformation of nicotinamide adenine bound to flavin reductase P. *Protein Sci.* **8**: 1725–1732.

Tironi IG, van Gunsteren WF. 1994. A molecular dynamics simulation of chloroform. *Mol. Phys.* **83**: 381–403.

Tu S-C, Mager HIX. 1995. Biochemistry of bacterial bioluminescence. *Photochem. Photobiol.* **62**: 615–624.

Van Calenbergh S, Verlinde CL, Soenens J, De Bruyn A, Callens M, Blaton NM, Peeters OM, Rozenski J, Hol WG, Herdewijn P. 1995. Synthesis and structure-activity relationships of analogs of 2′-deoxy-2′-(3-methoxybenzamido)adenosine, a selective inhibitor of trypanosomal glycosomal glyceraldehyde-3-phosphate dehydrogenase. *J. Med. Chem.* **38**(19): 3838–3849.

van Gunsteren WF, Berendsen HJC. 1987. *Groningen Molecular Simulation (GROMOS) Library Manual*. Biomos, Groningen.

van Gunsteren WF, Berendsen HJC. 1990. Computer simulations of molecular dynamics: methodology, applications and perspectives in chemistry. *Angew. Chem. Int. Ed. Engl.* **29**: 992–1023.

Velick SF. 1958. Fluorescence spectra and polarization of glyceraldehyde-3-phosphate and lactic dehydrogenase coenzyme complexes. *J. Biol. Chem.* **233**: 1455–1467.

Verlinde CL, Callens M, Van Calenbergh S, Van Aerschot A, Herdewijn P, Hannaert V, Michels PA, Opperdoes FR, Hol WG. 1994a. Selective inhibition of trypanosomal glyceraldehyde-3-phosphate dehydrogenase by protein structure-based design: toward new drugs for the treatment of sleeping sickness. *J. Med. Chem.* **37**(21): 3605–3613.

Verlinde CL, Merritt EA, Van den Akker F, Kim H, Feil I, Delboni LF,

Mande SC, Sarfaty S, Petra PH, Hol WG. 1994b. Protein crystallography and infectious diseases. *Protein Sci.* **3**(10): 1670–1686.

Weast RC. 1975. *Handbook of Chemistry and Physics*, CRC Press, Cleveland, OH.

Weber G. 1957. *Nature* **180**: 1409–1410.

Zenno S, Koike H, Kumar AN, Jayaraman R, Tanokura M, Saigo K. 1996a. Biochemical characterization of NfsA, the *Escherichia coli* major nitroreductase exhibiting a high amino acid sequence homology to Frp, a *Vibrio harveyi* flavin oxidoreductase. *J. Bacteriol.* **178**(15): 4508–4514.

Zenno S, Koike H, Tanokura M, Saigo K. 1996b. Conversion of NfsB, a minor *Escherichia coli* nitroreductase, to a flavin reductase similar in biochemical properties to FRase I, the major flavin reductase in *Vibrio fischeri,* by a single amino acid substitution. *J. Bacteriol.* **178**(15): 4731–4733.

Zens AP, Bryson TA, Dunlap RB, Fisher RR, Ellis PD. 1976. Nuclear magnetic resonance studies of pyridine dinucleotides. 7.1 The solution conformational dynamics of the adenosine portion of nicotinamide adenine dinucleotide and other related purine containing compounds. *J. Am. Chem. Soc.* **98**(24): 7559–7564.

Zens AP, Williams TJ, Wisowaty JC, Fisher RR, Dunlap RB, Bryson TA, Ellis PD. 1975. Nuclear magnetic resonance studies on pyridine dinucleotides. II. Solution conformational dynamics of nicotinamide adenine dinucleotide and nicotinamide mononucleotide as viewed by proton T1 measurements. *J. Am. Chem. Soc.* **97**(10): 2850–2857.

Zhang R-g, Evans G, Rotella FJ, Westbrook EM, Beno D, Huberman E, Joachimiak A, Collart FR. 1999. Characteristics and crystal structure of bacterial inosine-5′-monophosphate dehydrogenase. *Biochemistry* **38**: 4691–4700.

